Journal of Sound and Vibration (2000) **235**(4), 671–684
doi:10.1006/jsvi.2000.2948, available online at http://www.idealibrary.com on IDEAL®

ADAPTIVE CONTROL FOR SOUND AND VIBRATION ATTENUATION: A COMPARATIVE STUDY

J. SHAW

Mechanical Engineering Department, Huafan University, Shihtin, Taipei, Taiwan, 223, Republic of China. E-mail: jshaw@huafan.hfu.edu.tw

(*Received* 1 *September* 1999, *and in final form* 28 *February* 2000)

Adaptive control is often applied to a disturbed system whose parameters may be uncertain or even time varying. In this paper, two standard adaptive feedback controllers, featuring both system identification and control in real time, are compared for active sound and vibration attenuation. The two adaptive feedback controllers to be compared are the (i) self-tuning regulator and (ii) plant disturbance canceler. In the plant disturbance canceler, two methods for the controller tuning and three dithering schemes for plant model identification are considered. A numerical simulation for active vibration isolation and experimental investigations for active sound and vibration attenuation of the two adaptive feedback controllers are carried out. Both numerical and experimental results show that the self-tuning regulator outperforms the plant disturbance canceler in terms of much more amounts of sound and vibration attenuation and much faster convergence rate.

1. INTRODUCTION

Feedback control with the fixed controller has been of popular use for a long time and its successful applications can be found in a wide variety of engineering disciplines. The controller is usually designed based on the knowledge of the controlled process (plant) and the known operating conditions. However, control with a fixed controller may not always give satisfactory performance as was originally designed. The difficulty arises because of the possible changing properties of controlled processes and their signals, parameter uncertainty, existence of unknown disturbances, and so on. Adaptive control is therefore needed in such systems to modify their behavior in accordance with the aforementioned conditions. It is well known that an adaptive control system can be characterized by two complementary processes: identification and control. In the process of identification, a suitable model is developed online that exhibits the same input/output characteristics of the controlled process. Based on the identified model and control/performance objective, the controller is updated and then a control action is generated and tested on the plant in the control process. In other words, the adaptive control system can be viewed as an automation of plant modelling and controller design, in which the plant model and controller are updated at each sampling period.

In this paper, two types of adaptive controllers with feedback configuration are to be compared for attenuating the undesirable sound or vibration of a disturbed system with uncertain and/or time-varying parameters. More specifically, the adaptive feedback control system should perform two functions: it learns about the controlled process online and in the mean time controls its behavior (sound or vibration attenuation in this study). Among the various types of adaptive feedback controllers that can possibly do the job are the

0022-460X/00/340671 + 14 $35.00/0

self-tuning regulator (STR) of Astrom and Wittenmark [1, 2] and the adaptive plant disturbance canceler (PDC) derived from Widrow and Walach [3] and Shaw [4]. The STR is the best-known and most popular adaptive control method, which is just a direct integration of an identification and a controller design algorithm in such a manner that the two processes proceed sequentially. On the other side, the PDC has various forms of structures due to the three possible dithering schemes for real-time plant identification and an offline [3] and an online [4] process for the controller tuning. Though the adaptive PDC has a quite different control architecture as the STR, it functions much the same as the STR, i.e., real-time plant modelling and controlling. Therefore, it is of interest to compare performance of the two adaptive control systems in the context of active sound and vibration control.

This paper is organized as follows. In the next two sections the STR and adaptive PDC are briefly introduced, in which adaptive algorithms for real-time plant modelling and controller tuning are given and the three possible dithering schemes for online plant identification of the PDC are also included. In the Section 4 both adaptive feedback controllers are evaluated for active vibration isolation of a linear mechanical system by numerical simulation. Experimental investigation of the two adaptive feedback controllers applied to a system composed of two magnetostrictive actuators for active vibration isolation is conducted in Section 5. Active sound reduction in a duct by the two adaptive feedback controllers is experimentally examined in Section 6. Finally, conclusions of the paper are presented in Section 7.

2. DESCRIPTION OF THE SELF-TUNING REGULATOR

In this paper, a linear system with uncertain-but-fixed system parameters is to be disturbed by an unknown excitation $d(t)$ and to be controlled by an actuating signal $u(t)$. The two adaptive feedback controllers mentioned previously are thus employed for this plant disturbance attenuation. Figure 1 depicts the first adaptive control architecture, which is a generic diagram of the STR of Astrom and Wittenmark [1, 2]. The STR works in the following way. The plant output $y(t)$ contains a response to actuating signal $u(t)$, plus a response to plant disturbance $d(t)$. A plant estimator, receiving both the actuating signal and the plant output, estimates the plant parameters. These estimates are then fed to an automatic design algorithm that sets the parameters of the controller. Note that many different identification schemes have been developed. Among these the recursive least-squares (RLS) [5] algorithm has proved to be the most useful and practically successful self-tuning identifier. Note also that it is possible to parameterize the plant directly in terms of the control law parameters. If this is done, the design calculation necessary to determine the control law becomes essentially trivial. That is, direct adaptive algorithm is adopted.

In this paper, the plant is to be described by an ARMAX model [5] (i.e., a stochastic auto-regressive moving-average model):

$$A(q^{-1})y(t) = q^{-1}B(q^{-1})u(t) + C(q^{-1})d(t), \tag{1}$$

where $y(t)$, $u(t)$, and $d(t)$ are sequences of plant output, actuating signal, and disturbance, respectively, and A, B, and C are the corresponding polynomials of delay operator q^{-1} of appropriate orders. It can be shown [5] that the optimal one-step-ahead predictor for this model has the following form:

$$C(q^{-1})\hat{y}(t+1) = \alpha(q^{-1})y(t) + \beta(q^{-1})u(t), \tag{2}$$

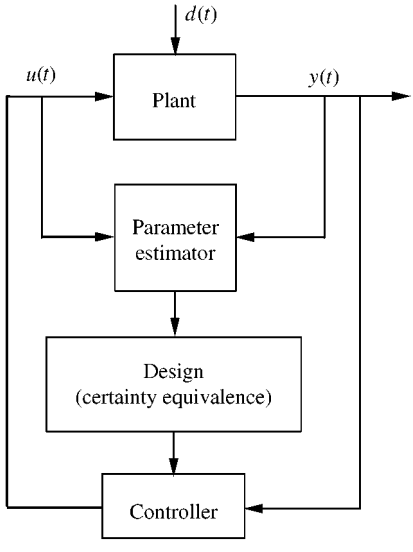

Figure 1. The STR control architecture.

where

$$\hat{y}(t+1) = y(t+1) - d(t+1) \tag{3}$$

is the optimal one-step-ahead prediction of $y(t)$. The RLS algorithm for plant parameter estimation and the minimum variance controller developed in reference [6] are adopted for the STR. The basic idea behind the controller is to form an adaptive prediction of the plant output and then to determine the atuating signal by setting the prediction output equal to the desired output. This is essentially the same philosophy as the one-step-ahead controller. Specifically, the RLS algorithm for system parameter estimation is as follows:

$$\theta(t) = \theta(t-1) + \frac{P(t-2)\phi(t-1)}{1 + \phi(t-1)^{\mathrm{T}} P(t-2)\phi(t-1)} [y(t) - \hat{y}(t)],$$

$$\hat{y}(t) = \phi(t-1)^{\mathrm{T}} \theta(t-1),$$

$$P(t-1) = P(t-2) - \frac{P(t-2)\phi(t-1)\phi(t-1)^{\mathrm{T}} P(t-2)}{1 + \phi(t-1)^{\mathrm{T}} P(t-2)\phi(t-1)} \tag{4}$$

with initially

$$\theta(0) = \mathbf{0}, \qquad P(-1) = \delta \mathbf{I}, \quad 0 < \delta < \infty. \tag{5}$$

Note that in equation (4)

$$\theta(t-1) = [\alpha_1(t-1), \cdots, \alpha_n(t-1), \beta_1(t-1), \cdots, \beta_m(t-1), c_1(t-1), \cdots, c_\ell(t-1)]^{\mathrm{T}} \tag{6}$$

and

$$\phi(t-1) = [y(t-1), \cdots, y(t-n), u(t-1), \cdots, u(t-m), -\hat{y}(t-1), \cdots, -\hat{y}(t-\ell)]^{\mathrm{T}} \tag{7}$$

are the respective estimated plant parameter vector and regression vector composed of the selected plant output, actuating signal, and the prediction variables. For the one-step-ahead controller, the control law based on minimum variance is hence

$$\phi(t)^{\mathrm{T}}\theta(t) = \hat{y}(t+1) = y^*(t+1) \tag{8}$$

from which the actuating signal can be obtained:

$$u(t) = \frac{1}{\beta_1(t)}\left[y^*(t+1) - \alpha_1(t)y(t) - \cdots - \beta_2(t)u(t-1) - \cdots + c_1(t)\hat{y}(t) + \cdots\right]. \tag{9}$$

Note that the desired output $y^*(t)$ is of course identically zero for the purpose of plant disturbance attenuation. The adaptive algorithms of equations (4)–(9) can hence be further simplified by removing $\hat{y}(t)$, $\hat{y}(t-1), \cdots$ and $c_1(t)$, $c_2(t), \cdots$ in $\phi(t)$ and $\theta(t)$, since

$$\phi(t)^{\mathrm{T}}\theta(t) = \hat{y}(t+1) = y^*(t+1) = 0 \quad \text{for all } t. \tag{10}$$

Note also that there is a remote possibility of division by zero in equation (9), which can be avoided by imposing constraint on the size of $\beta_1(t)$. This is done as follows, by assuming the knowledge of the sign and lower bound on the magnitude of β_1:
If

$$\beta_1(t)\operatorname{sign}\beta_1 < |\beta_1|_{min} \tag{11}$$

then

$$\beta_1(t) = |\beta_1|_{min}\operatorname{sign}\beta_1. \tag{12}$$

Another important practical point is that the actuating signal in equation (9) can call for large signal due to any large change in system parameters or in $y^*(t)$. In this case, the control law can be modified as follows:

$$\text{if } u(t) > u_{max} \quad \text{then } u(t) = u_{max},$$

$$\text{if } u(t) < u_{min} \quad \text{then } u(t) = u_{min},$$

where u_{max} and u_{min} are the specified maximum and minimum actuating signal levels.

3. DESCRIPTION OF THE PLANT DISTURBANCE CANCELER

Another adaptive feedback controller that can attenuate plant disturbance is the plant disturbance canceler by Widrow and Walach [3], as shown in Figure 2. Online plant modelling is achieved by introducing an external dither $\delta(t)$ to the system and the controller is tuned by an offline adaptive algorithm (another dither signal is used). Widrow and Walach have shown that no other linear system, regardless of its configuration, can reduce the variance of the plant disturbance to a level lower than that of Figure 2. In fact, it can be readily shown [4] that the transfer function from disturbance $d(t)$ to plant output response $y(t)$ is identically zero if the plant model and controller exactly match the plant actuation dynamics (namely from $u(t)$ to $y(t)$) and its inverse, respectively. More specifically, the plant

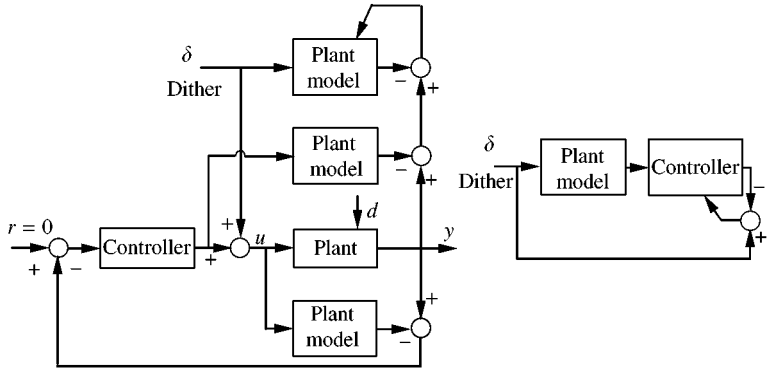

Figure 2. The PDC with offline controller tuning and scheme C.

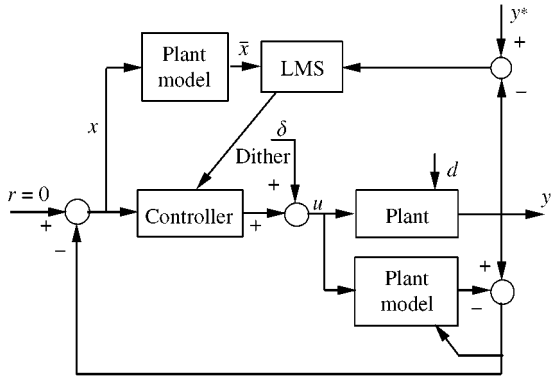

Figure 3. The PDC with online controller tuning and scheme A.

output response subtracted from the plant model output represents response of the system due to disturbance only. By utilizing this response, the controller is then used to compute the negating force $u(t)$ to negate effects of the disturbance on the plant. Complete plant disturbance attenuation can thus be achieved.

There are, however, other forms of adaptive PDC due to the three possible dithering schemes for plant modelling [3] and an online controller tuning method [4]. These are shown in Figures 3–5, which are just combinations of the three possible dithering schemes for plant modelling [3] and an online controller tuning method of filtered-x LMS algorithm [4]. Among the three possible dithering schemes for plant modelling, scheme A (see Figure 3) has the simplest form which is effective when the controller output is a stationary stochastic process and an independent dither is added to achieve a desired spectral character for the plant actuating signal $u(t)$. However, when the controller output is non-stationary (which is truly the case with the PDC architecture), one may be better off not including it at all in the plant modelling process. This is why dithering schemes B and C (see Figures 4 and 5) are introduced, since both use an independent dither exclusively in effecting the adaptive plant modelling process. The purpose is to assure known stationary statistics for the input modelling signal. Using scheme B with a white dither, the mean-square error will be minimized when the impulse response of the adaptive plant model exactly matches that of the plant over the duration span of the model's impulse response. However, it is

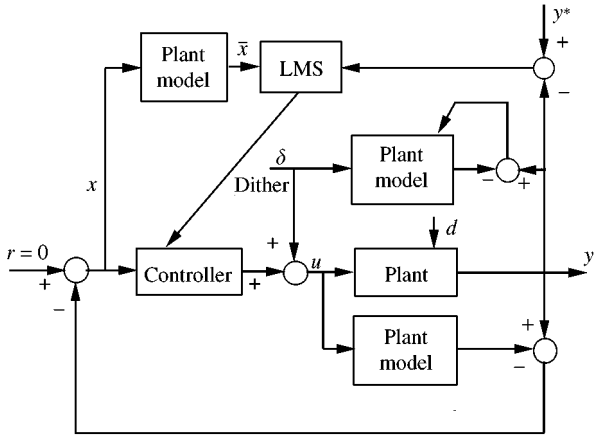

Figure 4. The PDC with online controller tuning and scheme B.

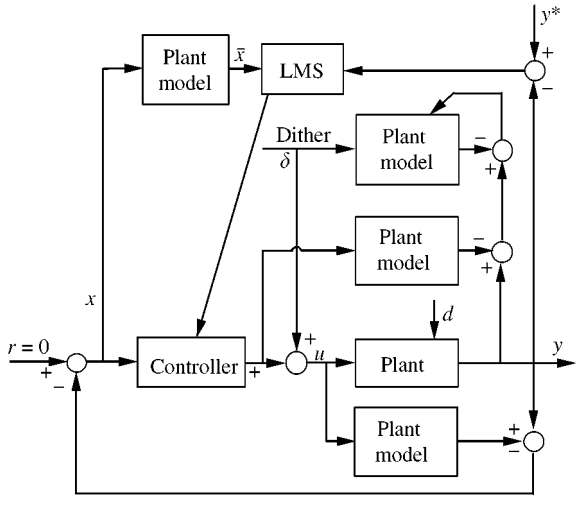

Figure 5. The PDC with online controller tuning and scheme C.

noted that dithering scheme B has larger minimum mean-square error at the adaptive plant model output than scheme A has, due to the additional power of the controller output after propagating through the plant. To compensate for this power, an extra plant model with controller output as the input signal needs to be included, as shown in scheme C. Scheme C thus has all the good features of scheme B and overcomes the drawback of having an increased minimum mean-square error, at the expense of increased system complexity.

To have a common ground for later comparison, the plant model in the PDC of Figures 2–5 is chosen the same ARMAX model as in the STR with the same total number of auto-regressive (n) and moving-average (m) coefficients. In addition, the RLS algorithm of equations (4) and (5) is used for tuning its coefficients online. For the controller model in the PDC, a finite impulse response (FIR) filter with length ℓ is adopted. As for the controller tuning, a direct least-mean-square (LMS) algorithm [7] is used offline in Figure 2, while a filtered-x LMS algorithm is employed online in Figures 3–5 which is re-introduced as follows [4].

Define the sum of squared error at the plant output at time step $k+1$ as

$$E(k+1) = \frac{1}{2}\sum_{i=1}^{k+1} e(i)^2 = \frac{1}{2}\sum_{i=1}^{k+1} (y^*(i) - y(i))^2 \tag{13}$$

which is also the error surface to be minimized. The desired response $y^*(i)$ is, of course, a zero response for plant disturbance attenuation. Minimization of the error function $E(k+1)$ is done by the method of steepest descent, which makes each change of the weights proportional to the negative of the gradient vector:

$$g_j(k+1) - g_j(k) = -\eta \frac{\partial E(k+1)}{\partial g_j(k)}, \quad j = 0, 1, \ldots, \ell - 1, \tag{14}$$

where $g_j(k)$ are the weights of the controller filter at time step k and η is a learning rate controlling the rate of convergence of the adaptive algorithm. Expanding the differentiation by using a series of chains rules yields

$$\begin{aligned} g_j(k+1) &= g_j(k) + \eta(y^*(k+1) - y(k+1)) G_u(z) x(k-j) \\ &= g_j(k) + \eta(y^*(k+1) - y(k+1)) \bar{x}(k-j), \end{aligned} \tag{15}$$

where $G_u(z)$ is the z-transform of the transfer function of the plant from $u(t)$ to $y(t)$ and $x(k)$ is the input sequence to the controller. The adaptation process of equation (15) is named a filtered-x LMS algorithm where

$$\bar{x}(k-j) = G_u(z) x(k-j) \tag{16}$$

is the filtered signal of $x(k)$ passing through the plant. However, the signal $\bar{x}(k)$ cannot be obtained in practice. Instead, it can be approximated by passing $x(k)$ through the plant model filter as shown in Figures 3–5, since the plant model filter is assumed to converge accurately to the plant dynamics as time goes by.

4. A NUMERICAL EXAMPLE FOR VIBRATION ISOLATION

A linear mass–spring–damper system with an attached active dynamic isolator [8] is taken as the plant under study and is shown in Figure 6. An external disturbance $d(t)$ applies at the main mass of the system and causes vibratory oscillation at the secondary mass. The attached mass–spring–damper–actuator system acts as a vibration isolator if the control goal is to minimize the vibrational amplitude at $y(t)$, namely, the undesirable vibration originated from the main mass is isolated from reaching the secondary mass. The power source injected into the actuator for providing control force can be either hydraulic or electromagnetic power source. For numerical simulation of the system, the following non-dimensionalized parameters are assumed:

$$m1 = 1, \qquad m2 = 0{\cdot}2, \qquad k1 = k2 = 1, \qquad b1 = b2 = 0{\cdot}1 \tag{17}$$

The two adaptive feedback controllers of STR and PDC described previously are employed for vibration isolation. For the plant model in both adaptive controllers, an

ARMAX model with $n = m = 11$ is taken. An FIR filter with $\ell = 150$ is chosen as the controller model in the adaptive PDC. A sampling period set at $\Delta T = 0{\cdot}05$ and the unknown disturbance $d(t)$ for the first mode excitation are used for all the following numerical simulation for vibration isolation. Note that zero initial coefficients (or weights) for the plant and controller models are adopted for both adaptive controllers in accordance with the presumed uncertain system parameters.

The adaptive controllers of Figures 1–5 are employed for active vibration isolation of the system. Figures 7–11 give the corresponding results for vibration isolation. It is clearly seen

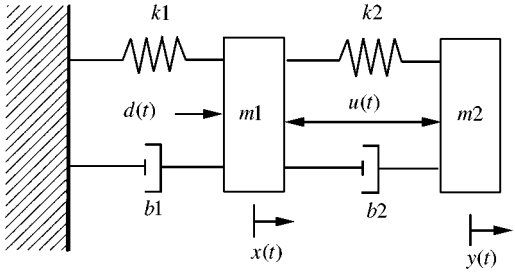

Figure 6. A mass–spring–damper system.

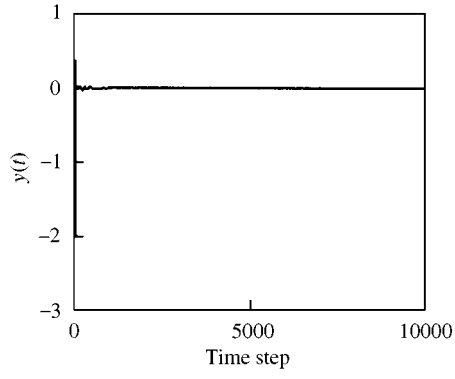

Figure 7. Vibration isolation by STR.

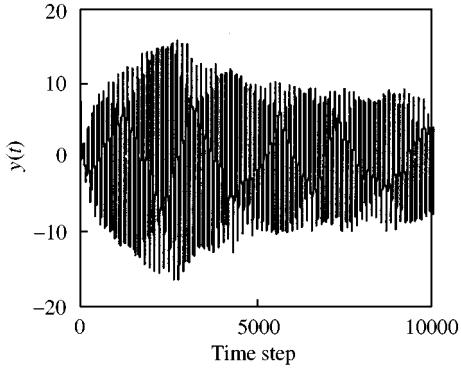

Figure 8. Vibration isolation by PDC with Figure 2 architecture.

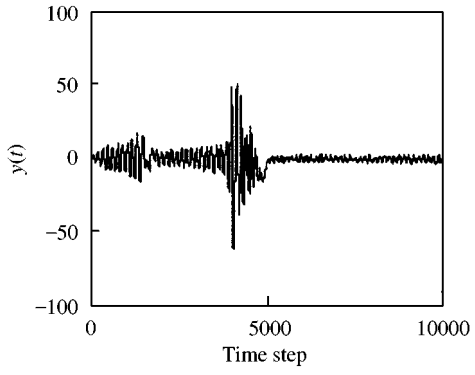

Figure 9. Vibration isolation by PDC with Figure 3 architecture.

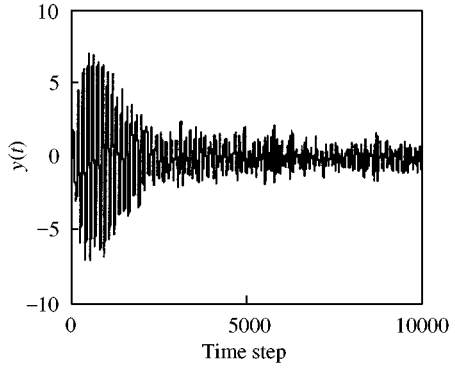

Figure 10. Vibration isolation by PDC with Figure 4 architecture.

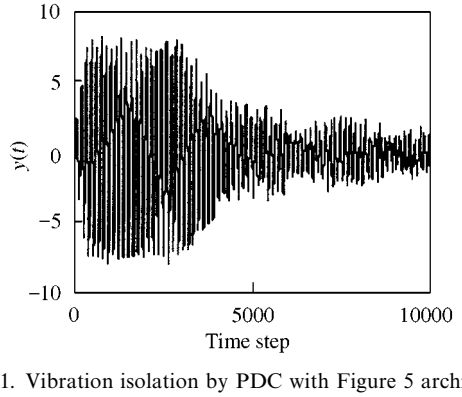

Figure 11. Vibration isolation by PDC with Figure 5 architecture.

that the STR of Figure 1 has the fastest convergence rate and obtains the most amounts of vibration isolation, while the PDC of Figure 2 has the worst performance. Note also that dithering schemes B and C have better overall performance over scheme A in the PDC, as readily seen in Figures 9–11. This is due to the fact that the controller output of dithering scheme A is non-stationary resulting in ineffective plant modelling. Table 1 summarizes the

final amounts of vibration amplitude isolated from reaching to the second mass of the five adaptive controllers at the end of 10 000 time-step running.

For this numerical example, the PDC of Figure 4 characterized by online filtered-x LMS algorithm for controller tuning and dithering scheme B for plant modelling gives the best performance over other PDC configurations. Therefore, it is adopted as the PDC that is going to be compared with the STR for both vibration and sound attenuation in the following two experiments. This is carried out next.

5. VIBRATION ISOLATION BY USING MAGNETOSTRICTIVE ACTUATOR

In this section, experiment investigations of the two adaptive controllers of STR and PDC for active vibration isolation by using magnetostrictive actuators are conducted. Figure 12 depicts the experimental set-up [4], which consists mainly of two magnetostrictive actuators. Magnetic field can induce strain in a magnetostrictive actuator. Therefore, an unknown magnetic field $d(t)$ provided by a power supply is applied to the lower actuator and vibratory oscillation at $y(t)$ of the upper actuator is recorded. The goal is to control the upper actuator so that the vibration amplitude $y(t)$ at the flat-top of the upper actuator is minimized, i.e., to maintain a quiescent flat-top in the presence of base vibrations.

An ARMAX model with $n = 1$ and $m = 31$ is adopted for modelling the actuator dynamics in both adaptive controllers. An FIR filter with $\ell = 60$ is chosen as the controller

TABLE 1

Vibration reductions in dB

STR (Figure 1)	PDC (Figure 2)	PDC (Figure 3)	PDC (Figure 4)	PDC (Figure 5)
40 dB	4·07 dB	12·58 dB	22·16 dB	18·56 dB

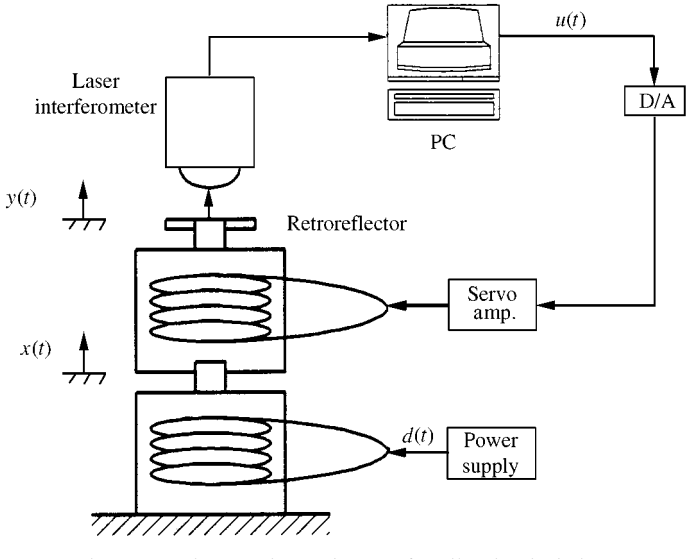

Figure 12. The experimental set-up for vibration isolation.

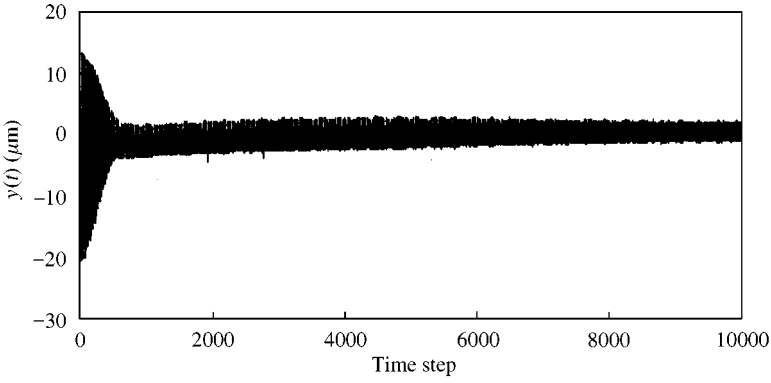

Figure 13. Time response for vibration isolation by STR.

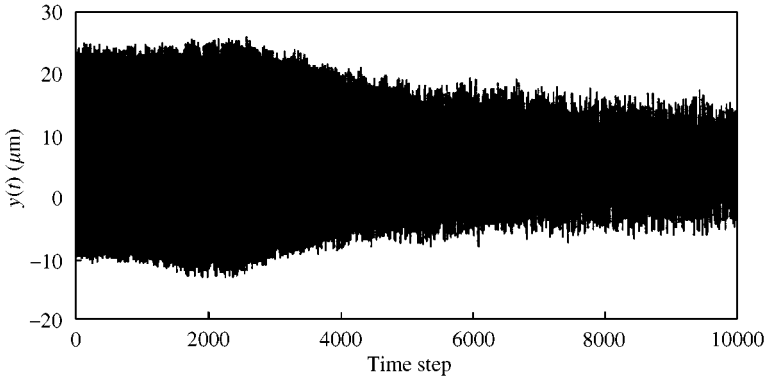

Figure 14. Time response for vibration isolation by PDC.

model in the adaptive PDC. A sampling rate set at 2 kHz and an unknown sinusoidal disturbance $d(t)$ at 60 Hz are used in the experiment. The control algorithms of the STR and PDC are digitally implemented in a 586 computer. For the dither signal in the PDC, a uniformly distributed random signal between ± 1 V is generated in the control program for the purpose of plant modelling. Again, zero initial coefficients (or weights) for the plant and controller models are adopted in accordance with the presumed unknown plant parameters. Figures 13 and 14 show the vibration control results of the STR and PDC respectively. The peak-to-peak vibration amplitude at $y(t)$ is attenuated from 34·56 to 3 μm by the STR and to 18 μm by the PDC at the end of 5 s running. Vibration reductions of 21·2 and 5·66 dB, respectively, is obtained by the STR and PDC, thus proving once more the STR outperforms the PDC in active vibration attenuation.

6. ACTIVE NOISE CONTROL IN DUCTS

In this section, the two adaptive controllers are to be tested on a well-publicized problem of active noise control in ducts. This problem has been widely studied from the early work of Leug [9] by feedforward control and work of Olson and May [10] by feedback control to the work of Eriksson and Allie [11] by both feedforward and feedback control. For a comprehensive coverage on the study of active control of noise propagating in ducts, the

reader is referred to the work of Hansen and Snyder [12]. The two adaptive controllers employed in this paper have such advantages of using only one sensor and one actuator and can adapt themselves in real time over other control methods appeared in the literature for this noise reduction problem. It is noted, however, that the sensor and actuator have been properly placed at locations in the duct where the controllability and observability of the problem are well preserved.

The experimental set-up for active sound reduction in a duct is shown in Figure 15. An unknown sinusoidal noise of 120 Hz generated by the primary loudspeaker is to be attenuated at the measurement microphone by superpositioning an interfering sound wave generated by the secondary loudspeaker. A low-pass filter with cut-off frequency of 300 Hz is installed after the D/A converter for smoothing the control signal. The sampling rate set for real-time plant modelling and controlling is 3 kHz. The two adaptive controllers are implemented in a 586 computer. It is noted that due to the speed limitation of the microcomputer, the RLS algorithm for plant parameter estimation in equations (4) and (5) is replaced by a less computation-demanding algorithm of the projection method [5]:

$$\theta(t) = \theta(t-1) + \frac{\eta\phi(t-1)}{1 + \phi(t-1)^{\mathrm{T}}\phi(t-1)}\,[y(t) - \hat{y}(t)], \tag{18}$$

$$\hat{y}(t) = \phi(t-1)^{\mathrm{T}}\theta(t-1),$$

where the constant η is a learning rate controlling the rate of convergence.

An ARMAX model with $n = 100$ and $m = 100$ for the plant model and an FIR filter with $\ell = 150$ for the controller are chosen in the adaptive PDC, whereas an ARMAX model with $n = 50$ and $m = 150$ is adopted for the STR in the experiment. Before conducting the experiment, all the initial coefficients for the modelling filters in both adaptive controllers are set to zeros. For the dither signal in the PDC, a uniformly distributed random signal between $\pm$ 0·5 V is generated in the control program for the purpose of plant modelling. Figures 16 and 17 show the noise reduction results of the two adaptive controllers. The amplitude of the sound pressure in the duct has been reduced from 1·125 to 0·0625 V by STR and from 0·86 to 0·14 V by PDC at the end of a 4 s operation. Equivalently, the sound pressure in the duct is reduced an amount of 32·7 dB by the STR and 17 dB by the PDC. It is shown again that the STR has a much better performance in attenuating the noise in

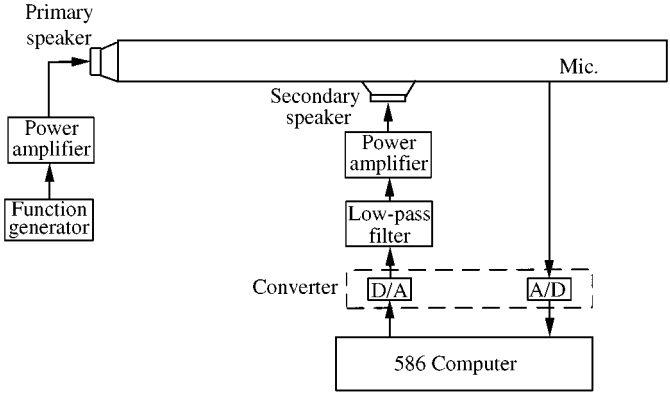

Figure 15. The experimental set-up for sound reduction in a duct.

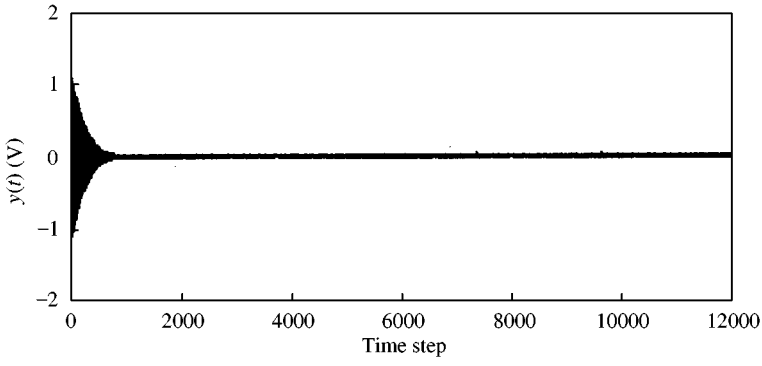

Figure 16. Time response for noise reduction by STR.

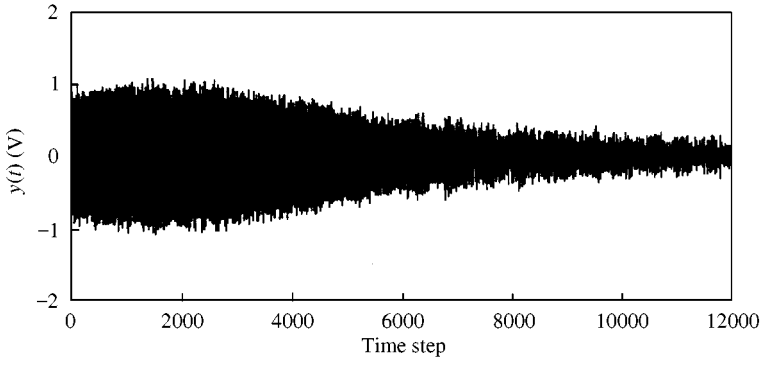

Figure 17. Time response for noise reduction by PDC.

a duct than the PDC. Note that this problem of active noise control in a duct had also been successfully solved by Eriksson and Allie [11] by an adaptive feedforward control, where two microphones are used and where online controller tuning by the filtered-x LMS algorithm and plant modelling by dithering scheme B are employed.

7. CONCLUSIONS

This paper is concerned with the comparison of the performance of two standard adaptive feedback control systems of the self-tuning regulator and plant disturbance canceler. Based on the results of both numerical and experimental evaluations of the two adaptive controllers applied to active noise and vibration control, the following conclusions are made.

1. The self-tuning regulator outperforms the plant disturbance canceler in terms of much more amounts of sound and vibration attenuation and much faster convergence rate in all the examples studied in this paper.
2. For the plant disturbance canceler, online fine-tuning of the controller with the filtered-x LMS algorithm seems superior than using the offline tuning process by the direct LMS algorithm (referring to Figures 8 and 10). The reason is that the online filtered-x LMS

algorithms aims to directly minimize the plant output for disturbance attenuation, while the offline process for tuning the controller aims to converge to the inverse plant model.

3. In the plant modelling process of the plant disturbance canceler, dithering schemes B and C (Figures 4 and 5), though having somewhat complex system configurations, improve on dithering scheme A (Figure 3) for the case when the controller output is non-stationary.
4. For the numerical example studied, the plant disturbance canceler of Figure 4 with the online filtered-x LMS algorithm for controller tuning and dithering scheme B for plant modelling gives the best performance over other plant disturbance canceler configurations.

Finally, it is pointed out that in this paper the self-tuning regulator and plant disturbance canceler are applied only to disturbed systems with uncertain-but-fixed system parameters. It is obvious that these adaptive feedback controllers can certainly be applied to a time-varying system since both plant modelling and controller tuning can be carried out online in a real-time scale. Moreover, only one sensor for measuring the system output is needed in both adaptive feedback controllers, as opposed by some feedforward controllers where multiple sensors are usually employed.

ACKNOWLEDGMENT

This work was supported by National Science Council, Taiwan, ROC, under grant number NSC 88-2212-E-211-001.

REFERENCES

1. K. J. Astrom and B. Wittenmark 1973 *Automatica* **9**, 195–199. On self-tuning regulators.
2. K. J. Astrom and B. Wittenmark 1995 *Adaptive Control*. Menlo Park, CA: Addison-Wesley, Second edition.
3. B. Widrow and E. Walach 1996 *Adaptive Inverse Control*. Englewood Cliffs, NJ: Prentice-Hall.
4. J. Shaw 1998 *Journal of Intelligent Material Systems and Structures* **9**, 87–94. Adaptive vibration control by using magnetostrictive actuator.
5. G. C. Goodwin and K. S. Sin 1984 *Adaptive Filtering Prediction and Control*. Englewood Cliffs, NJ: Prentice-Hall.
6. K. J. Astrom, U. Borisson, L. Ljung and B. Wittenmark 1977 *Automatica* **13**, 457–476. Theory and application of self-tuning regulators.
7. S. Haykin 1991 *Adaptive filter theory*. Englewood Cliffs, NJ: Prentice-Hall.
8. J. Shaw 1998 *Journal of Control Systems and Technology* **6**, 223–230. Active control of a vibration absorber/isolator by using a plant disturbance canceler.
9. P. Lueg 1936 *US Patent No.* 2043416. Process of silencing sound oscillations.
10. H. F. Olson and E. G. May 1953 *Journal of the Acoustic Society of America* **25**, 1130–1136. Electronic sound absorber.
11. L. J. Eriksson and M. C. Allie 1989 *Journal of the Acoustic Society of America* **85**, 797–802. Use of random noise for on-line transducer modeling in an adaptive active attenuation system.
12. C. H. Hansen and S. D. Snyder 1997 *Active Control of Noise and Vibration*. London, UK: E & Fn Spon, Chapter 7.